

Isoquinoline–pyridine-based protein kinase B/Akt antagonists: SAR and in vivo antitumor activity

Gui-Dong Zhu,^{a,*} Jianchun Gong,^a Akiyo Claiborne,^a Keith W. Woods,^a Viraj B. Gandhi,^a Sheela Thomas,^a Yan Luo,^a Xuesong Liu,^a Yan Shi,^a Ran Guan,^a Shayna R. Magnone,^a Vered Klinghofer,^a Eric F. Johnson,^a Jennifer Bouska,^a Alexander Shoemaker,^a Anatol Oleksijew,^a Vincent S. Stoll,^b Ron De Jong,^c Tilman Oltersdorf,^c Qun Li,^a Saul H. Rosenberg^a and Vincent L. Giranda^a

^aCancer Research, GPRD, Abbott Laboratories, Abbott Park, IL 60064, USA

^bStructural Biology, GPRD, Abbott Laboratories, Abbott Park, IL 60064, USA

^cIDUN Pharmaceuticals Inc., 9380 Judicial Drive, San Diego, CA 92121, USA

Received 22 February 2006; accepted 17 March 2006

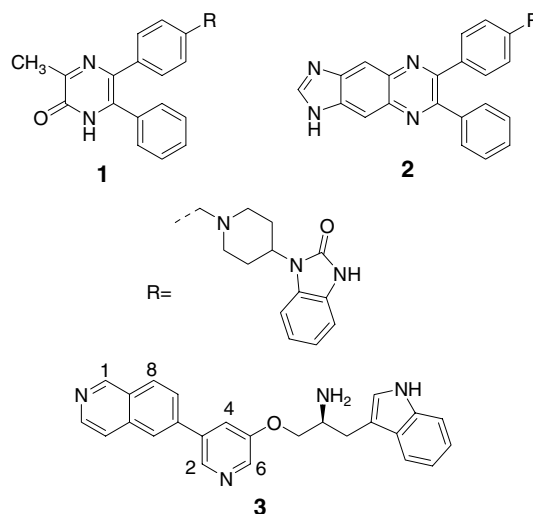
Available online 5 April 2006

Abstract—The structure–activity relationships of a series of isoquinoline–pyridine-based protein kinase B/Akt antagonists have been investigated in an effort to improve the major short-comings of the lead compound **3**, including poor pharmacokinetic profiles in several species (e.g., mouse iv $t_{1/2}$ = 0.3 h, po F = 0%). Chlorination at C-1 position of the isoquinoline improved its pharmacokinetic property in mice (iv $t_{1/2}$ = 5.0 h, po F = 51%) but resulted in >500-fold drop in potency. In a mouse MiaPaCa-2 xenograft model, an amino analog **10y** significantly slowed the tumor growth, however was accompanied by toxicity.

© 2006 Elsevier Ltd. All rights reserved.

Protein kinase B (also known as Akt) is a 57 kDa serine/threonine kinase that in mammals is comprised of three highly homologous isoforms, namely PKB α (Akt1), PKB β (Akt2), and PKB γ (Akt3).¹ The cellular activation of PKB/Akt triggers a cascade of responses, from cell growth and proliferation to survival and motility, driving tumor progression. Overexpression of Akt as a result of, for example, inactivation of tumor suppressor PTEN has been correlated with an increasing number of human cancers.² Therefore, inhibition of Akt alone, or in combination with other standard cancer chemotherapeutics, is widely considered as a practical strategy for the treatment of cancers.³ While initial development of small Akt inhibitors has been summarized in two review articles,³ Lindsley et al. recently reported a series of selective allosteric and non-ATP competitive diphenylquinoxaline- and diphenylpyridine-based inhibitors of Akt that target the pleckstrin homology (PH) domain of the protein kinase.⁴ Some of these Akt inhibitors (e.g., **1**) are selective over other members of the closely

related AGC family of protein kinases and displayed good selectivity among the individual Akt isozymes. An optimized dual Akt1/Akt2 inhibitor **2** was demonstrated to sensitize tumor cells to apoptotic stimuli and inhibit the phosphorylation of both Akt1 and Akt2 in vitro.⁵



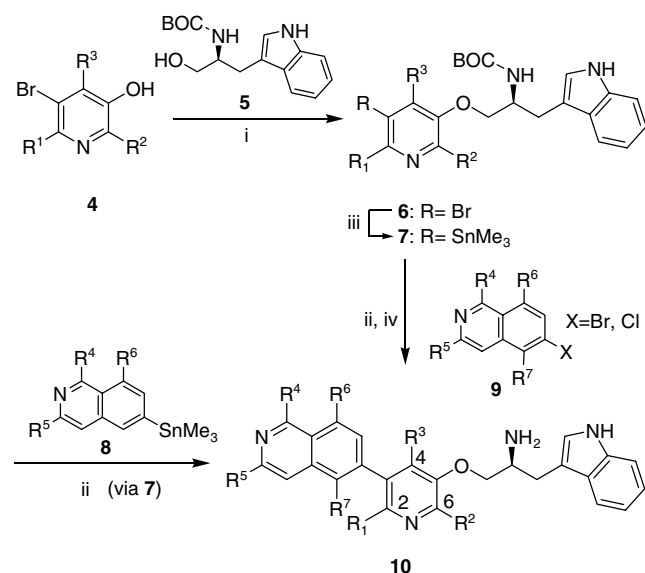
Keywords: Akt inhibitor; Protein kinase B; PKB; GSK3; FL5.12-Akt; Anticancer.

* Corresponding author. Tel.: +1 847 935 1305; fax: +1 847 935 5165; e-mail: gui-dong.zhu@abbott.com

We have reported a novel, potent ($IC_{50} = 2.0$ nM), and selective Akt inhibitor **3** that showed statistically significant efficacy in several mouse xenograft models.⁶ Major short-comings of this Akt inhibitor as a clinically useful agent include short half-life in mice, rat, and monkey, and a narrow therapeutic window. In an effort to improve the pharmacokinetic profile and retain potency against Akt, the structure–activity relationships of this class of Akt inhibitors have been investigated under the guidance of an X-ray structure of **3** bound to analogous protein kinase A (PKA).

Outlined in Scheme 1 is a general synthesis of the pyridine–isoquinoline-based Akt inhibitors. Mitsunobu coupling of 5-bromopyridin-3-ol **4** with *N*-Boc-tryptophanol (**5**) provided aryl ether **6**. Stille coupling with trimethylstannyl-isoquinoline **8** and Boc-deprotection afforded Akt inhibitors **10**. Alternately, the aryl bromide **6** was converted to the corresponding trimethylaryltin **7** by treatment with hexamethylditin in refluxing toluene under the catalysis of $Pd(PPh_3)_4$. Compounds **7**, under typical Stille conditions [$Pd_2(dba)_3/(o\text{-tol})_3P/DMF$], smoothly coupled with bromide **9** ($X = Br$). The reaction of **7** with commercially available 8-methyl-6-chloroisoquinoline **9** ($X = Cl$, $R^4 = R^5 = R^6 = H$), however, required the catalyst dicyclohexylphosphino-2'-(*N,N*-dimethylamino)-biphenyl (Cy-MAP). Boc-deprotection under acidic conditions provided Akt inhibitors **10**.

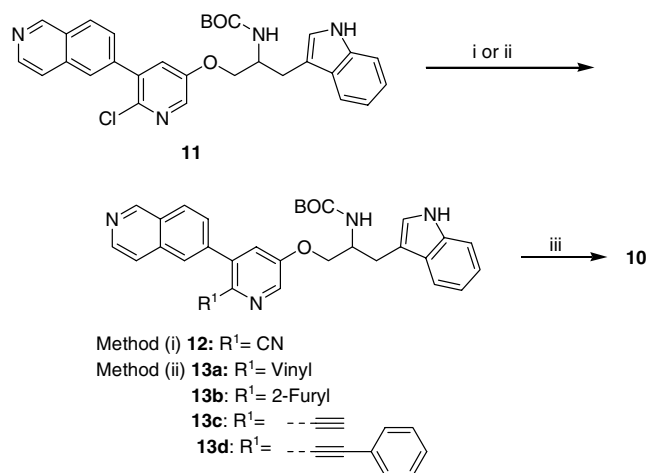
The C-2 position of the pyridine in **10** was modified through an intermediate chloride **11**, that was in turn prepared according to the general protocol described in Scheme 1 from 6-chloro-5-bromopyridin-3-ol **4** ($R^1 = Cl$, $R^2 = R^3 = H$).⁷ The cyanation of **11** under typical conditions [$Zn(CN)_2/Pd(Ph_3)_4/DMF$] required more than 3 days heating at 90 °C, providing cyanide **12** in



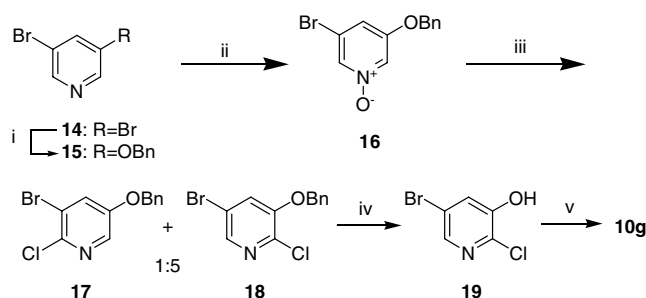
Scheme 1. Reagents and conditions: (i) DEAD, Ph_3P , THF. (ii) a— $Pd_2(dba)_3$, $P(o\text{-tol})_3$, DMF; b— CF_3CO_2H , CH_2Cl_2 ; (iii) $Pd(PPh_3)_4$, $Me_3SnSnMe_3$, toluene, 110 °C, 3 h, 85%; (iv) a—2-Dicyclohexylphosphino-2'-(*N,N*-dimethylamino)biphenyl, $Pd_2(dba)_3$, Et_3N , DMF; b— CF_3CO_2H , CH_2Cl_2 .

89% yield (Scheme 2). The Stille coupling of **11** with 2-tributylstannylfuran went smoothly with Cy-MAP as ligand, giving the coupled product **13b** in 75% yield. However, a similar reaction with tributylvinyltin provided only 26% of desired product **13a**. Likewise, the reaction of **11** with tributyl(ethynyl)tin in the presence of $Pd_2(dba)_3$ and Cy-MAP furnished **13c** in 20% yield. When the tributylstannylethynyl C–H was substituted with a phenyl group, reaction with **11** under the same conditions afforded **13d** in 96% yield.

Incorporation of a chlorine at the C-6 position of the pyridine is described in Scheme 3. 5-Bromo-3-benzyl-oxy-pyridine (**15**), prepared from dibromopyridine **14** in 75% yield, was oxidized with *m*-CPBA to afford *N*-oxide **16**. Chlorination of **16** with $POCl_3$ provided a mixture of **17** and **18** with the desired chloride **18** predominating. The regio-chemistry of the two isomers was determined by comparison of de-benzylated material (30% HBr in HOAc) with an authentic sample of **4** ($R^1 = Cl$, $R^2 = R^3 = H$).⁷ The chloride **19** was converted to **10g** by the standard protocol as shown in Scheme 1 in 30% overall yield.



Scheme 2. Reagents: (i) $Zn(CN)_2$, $Pd(PPh_3)_4$, DMF, 89%; (ii) $Pd_2(dba)_3$, dicyclohexylphosphino-2'-(*N,N*-dimethylamino)biphenyl (Cy-MAP), Et_3N , DMF; (iii) CF_3CO_2H , CH_2Cl_2 .



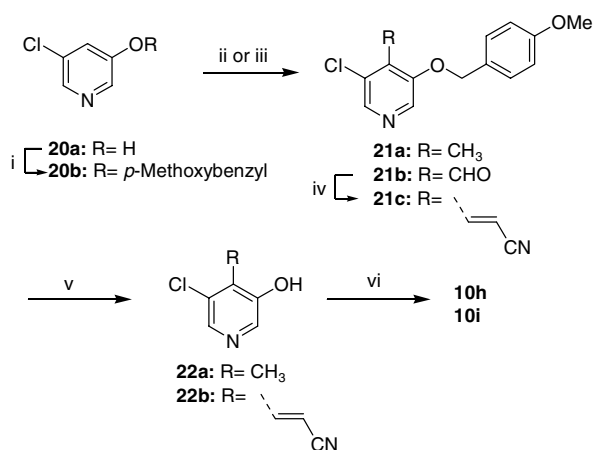
Scheme 3. Reagents: (i) $BnOH$, NaH , DMF, 75%; (ii) *m*-CPBA, CH_2Cl_2 , 100%; (iii) $POCl_3$, CH_2Cl_2 , 61%; (iv) HBr, HOAc, 84%; (v) a—Tryptophanol, DEAD, Ph_3P , THF, 70%; b—**8** ($R^4 = R^5 = R^6 = H$), $Pd_2(dba)_3$, $P(o\text{-tol})_3$, DMF; c— CF_3CO_2H , CH_2Cl_2 , 44% over two steps.

The C-4 position of the pyridine was alkylated or acylated in good to excellent yields through lithiation of chloride **20b** with LDA followed by treatment with iodomethane or methyl formate (Scheme 4). A similar reaction with bromide **15** failed to provide any product. Wittig olefination of the aldehyde **21b** with diethylphosphonoacetonitrile afforded **21c**. The *para*-methoxybenzyl protecting group in **21c** was cleaved in refluxing trifluoroacetic acid to give **22**. Conversion to **10h** and **10i** was carried out by standard procedures as described in Scheme 1.

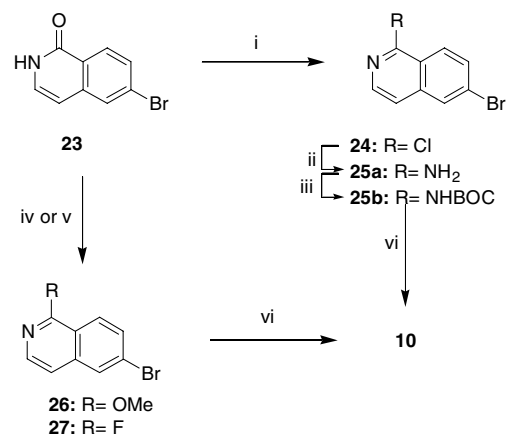
Modification at C-1 position of the isoquinoline is described in Scheme 5, starting from 6-bromo-isoquinolinone **23**.⁸ Treatment of **23** with POCl₃ at reflux provided chloride **24** which was converted to the amine **25**. O-methylation of isoquinolinone **23** was conducted under Mitsunobu conditions. 1-Fluoroisoquinoline **27** was obtained in an average of 15% yield in several attempts through heating **23** with commercially available perfluoro-2-methyl-2-pentene and triethylamine in acetonitrile in a sealed tube. Stille coupling of **24–27** with trimethylstannyl **7**, followed by Boc-deprotection, gave the Akt inhibitors **10j–10n**.

Syntheses of 3-substituted isoquinoline analogs **10p–10y** are depicted in Scheme 6. 3-Chloro-6-bromoisoquinoline **28** and 3-amino-6-bromoisoquinoline **29** were prepared according to literature procedures.⁹ Sandmeyer reaction of 3-aminoisoquinoline **29**, followed by treating with 70% hydrogen fluoride in pyridine, furnished 3-fluoro-analog **30**. Stille coupling of **28**, **29**, and **30** with trimethylstannyl **7** gave compounds **31**, **32**, and **33**.

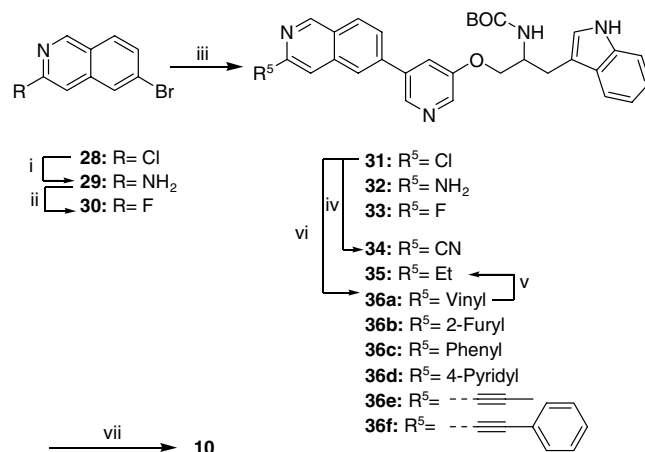
The 3-chloro-functionality in compound **31** was readily replaced with cyano to give **34** under the same cyanation condition as detailed in Scheme 2. The Stille reaction of



Scheme 4. Reagents: (i) DEAD, Ph₃P, CH₂Cl₂, 87%; (ii) LDA, MeI, THF, 65%; (iii) LDA, HCO₂Me, THF, 78%; (iv) (EtO)₂P(O)CH₂CN, LiHMDS, THF, 95%; (v) CF₃CO₂H, 95%; (vi) a—*N*-Boc-tryptophanol, DEAD, Ph₃P, THF, 70% for **22a**, 60% for **22b**; b—**8** (R⁴ = R⁵ = R⁶ = H), Pd₂(dba)₃, 1,3-bis(2,6-di-*i*-propylphenyl)imidazolium chloride, DMF, 32% for **22a**, 48% for **22b**; c—CF₃CO₂H, CH₂Cl₂, 81% for **22a**, 80% for **22b**.



Scheme 5. Reagents and conditions: (i) POCl₃, 100 °C, 4 h., 62%; (ii) Acetamide, K₂CO₃, 180 °C, 5 h., 65%; (iii) (Boc)₂O, DMAP, Et₃N, MeCN; (iv) DEAD, Ph₃P, THF, 62%; (v) Perfluoro-2-methyl-2-pentene, Et₃N, MeCN, 15%; (vi) a—**7**, Pd₂(dba)₃, P(*o*-tol)₃, DMF; b—CF₃CO₂H, CH₂Cl₂.

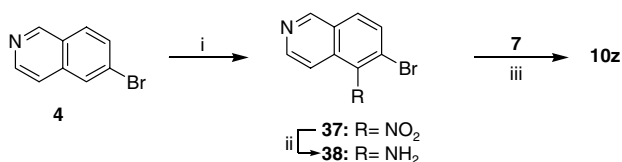


Scheme 6. Reagents: (i) a—NaH, BnNH₂, DMF, 42%; b—CF₃CO₂H, reflux, 66%; (ii) NaNO₂, HF/pyridine, 92%; (iii) **7**, Pd₂(dba)₃, (*o*-tol)₃P, Et₃N, DMF, 75%; (iv) Zn(CN)₂, Pd(PPh₃)₄, DMF, 71%; (v) H₂, 10% Pd/C, 30%; (vi) Pd₂(dba)₃, dicyclohexylphosphino-2'-(*N,N*-dimethylamino)biphenyl (Cy-MAP1), Et₃N, DMF; (vii) CF₃CO₂H, CH₂Cl₂.

31 with a variety of tin reagents, under the catalysis of Cy-MAP, provided **36a–36f**. Hydrogenation of **36a** in the presence of 10% palladium on carbon afforded **35**. Boc-deprotection of **31–36f** under acidic conditions provided **10o–10y**.

Nitration of 6-bromoisoquinoline **4** (R⁴ = R⁵ = R⁶ = R⁷ = H) with concentrated nitric acid in concentrated sulfuric acid regio-specifically afforded 5-nitroisoquinoline **37** (Scheme 7). No other isomer was detected by either HPLC analysis or ¹H NMR of the crude product. Reduction of the nitro-compound with iron dust in acetic acid provided amino analog **38** which was converted to **10z** through Stille coupling and Boc-deprotection.

Illustrated in Figure 1 is a depiction of the X-ray structure of **3** in PKA, a closely related protein kinase of Akt in the same AGC family.^{3,6} Corresponding residues for



Scheme 7. Reagents: (i) 63% HNO_3 /96% H_2SO_4 , 88% yield; (ii) Fe, $\text{HOAc}/\text{H}_2\text{O}$, 92%; (iii) a— $\text{Pd}_2(\text{dba})_3$, $\text{P}(o\text{-tol})_3$, Et_3N , DMF, 60%; b— $\text{CF}_3\text{CO}_2\text{H}$, CH_2Cl_2 , 66%.

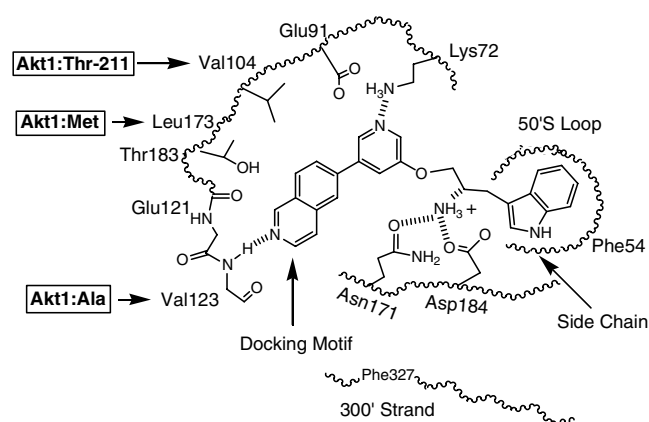


Figure 1. An illustration of the X-ray structure of **3** bound to PKA.

Akt in the ATP-binding site are shown on the left. As shown in Figure 1, three sets of hydrogen bonds of **3** to Val-123, Lys-72, and Asn-171/Asp-184 are critical for its high potency against PKA ($\text{IC}_{50} = 2.1 \text{ nM}$). The hydrophobic indole moiety in **3** fits nicely underneath the glycine-rich loop. Our initial goal was to optimize the physico-properties of **3** through substitution on the pyridine and isoquinoline rings, keeping the remainder of molecule unchanged. The appropriate substituents may also pick up additional interactions (e.g., with Thr-211 in Akt) and lead to more potent and Akt-selective analogs. In addition, **10k** has been characterized as a major metabolite of **3** in most species and this metabolism of **3** was attributed to its short half-life (e.g., 0.3 h in mice). Therefore, substitution at the C-1 position of the isoquinoline could block this metabolism. From the X-ray structure, the space between Glu-121 and the isoquinoline is rather limited, so the group introduced at the C-1 position required to be relatively small.

SAR studies of analogs of **3** modified at the *ortho*- and *para*-positions of the central pyridine are summarized in Table 1. Illustrated by examples **10a–10e**, relatively small groups are tolerated at the C-2 position of the pyridine. No significant impact from a weakly electron-withdrawing group (e.g., chlorine) was observed at this position (**10a**), while introduction of a strongly electron-withdrawing functionality such as a cyano group is detrimental to its activity (**10b** vs **10e**). Relatively larger groups, even with a linear linker (**10f**), led to a much less potent Akt inhibitor. Introduction of a chlorine at the C-6 position of the pyridine (**10g**) resulted in 6-fold drop in Akt activity ($\text{IC}_{50} = 12 \text{ nM}$). An even more dramatic reduction in potency was observed by introduc-

Table 1. Enzyme assay results for compounds **3** and **10a–10i** against Akt

Compound	R ¹	R ²	R ³	Akt1 IC_{50}^a (nM)
3	H	H	H	2.0
10a	Cl	H	H	1.8
10b	CN	H	H	4.6
10c	—	H	H	2.0
10d	—	H	H	1.5
10e	—	H	H	0.8
10f	—	H	H	1240
10g	H	Cl	H	12
10h	H	H	CH ₃	84
10i	H	H	—	697

^a Values are means of two or more experiments. Unless otherwise specified, all compounds were tested at 5 μM ATP.

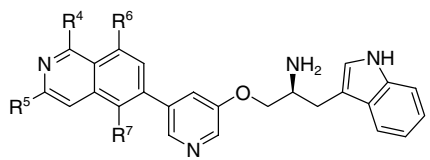
tion of a methyl (**10h**) or acrylonitrile (**10i**) group at the C-4 position of the pyridine ($\text{IC}_{50} = 84$ and 697 nM, respectively).

As revealed in Table 2, any modification at the C-3 position of the isoquinoline led to more than two orders of magnitude loss in potency against Akt. This reduced potency seems to correlate with the size of the substituents, less for fluorine analog (**10j**; $\text{IC}_{50} = 227 \text{ nM}$) and more for chlorine (**10l**; $\text{IC}_{50} = 778 \text{ nM}$) and methoxy group (**10m**; $\text{IC}_{50} = 39,500 \text{ nM}$). Possible interaction of an amino group with Val-123 backbone carbonyl is possibly responsible for the modest potency of amino analog **10n** ($\text{IC}_{50} = 160 \text{ nM}$).

Substituents are significantly better tolerated at the C-3 position of the isoquinoline scaffold. No obvious correlation was observed though between activity and either sterics or electronics of the substituents (**10o–10y**). It is likely that a combination of factors involved in the protein–ligand binding, including inhibitor-induced conformational change of the protein (i.e., **10x**; $\text{IC}_{50} = 56 \text{ nM}$) and formation of additional interaction with the protein (i.e., **10y**; $\text{IC}_{50} = 3.4 \text{ nM}$).

Introduction of an amino group at the 5-position of the isoquinoline resulted in a nearly 10-fold drop in its Akt activity (**10z**). In an effort to reduce the metabolic liability at the C-1 position of the isoquinoline through a 1,8-steric interaction, a methyl group was installed at the C-8 position. However, the 500-fold drop in the potency of **10aa** suggests a limited space between the isoquinoline and the hinge protein backbone.

Summarized in Table 3 is the selectivity profile of selected Akt inhibitors with representative substituents on the pyridine and isoquinoline rings. Like compound **3**, all inhibitors, except for **10y**, displayed from modest to

Table 2. Enzyme assay results for compounds **3** and **10j–10aa** against Akt


Compound	R ⁴	R ⁵	R ⁶	R ⁷	Akt1 IC ₅₀ ^a (nM)
3	H	H	H	H	2.0
10j	F	H	H	H	227
10k	OH	H	H	H	1240
10l	Cl	H	H	H	778
10m	OMe	H	H	H	39,500
10n	NH ₂	H	H	H	160
10o	H	F	H	H	3.5
10p	H	Cl	H	H	407
10q	H	CN	H	H	640
10r	H	Et	H	H	144
10s	H	—	H	H	22
10t	H	—	H	H	57
10u	H	Ph	H	H	305
10v	H	—	H	H	122
10w	H	—	CH ₃	H	180
10x	H	—	Ph	H	56
10y	H	NH ₂	H	H	3.4
10z	H	H	H	NH ₂	15
10aa	H	H	CH ₃	H	995

^a Values are means of two or more experiments. All compounds were tested at 5 μ M ATP.

Table 3. Selectivity profile of selected Akt inhibitors in comparison to **3** (IC₅₀^a, nM)

Kinase	3	10a	10e	10o	10y
Akt1	2.0	1.2	0.8	3.5	3.4
Akt2	6.8	5	5	nd ^b	21
Akt3	35	73	39	nd	76
PKA	2.1	5	1	48	8
PKC γ	270	540	260	nd	31
PKC ξ	6,100	>5000	8900	nd	8300
CDK1	100	870	4900	3400	22
ERK2	910	37,000	27,200	nd	1200
CK2	11,800	12,700	>50,000	nd	620
SRC	2000	12,100	>50,000	18,000	480

^a All compounds were tested at 5 μ M ATP.

^b Not determined.

excellent selectivity against different families of protein kinases. Installation of small groups at the C-2 position of the pyridine as exemplified by **10a** and **10e** improves selectivity over some of the kinases such as CDK1, while 3-amino analog **10y** was generally less selective.

Phosphorylation of the Akt downstream targets such as GSK α/β was measured in the presence of inhibitors as an indication of their Akt inhibitory activity in cells. Anti-proliferative activities of the majority of our Akt

Table 4. Cellular activity of selected Akt inhibitors in comparison to **3** (IC₅₀^a, μ M)

Cell	3	10a	10e	10o	10y
GSK3-P	1.5	3.0	nd ^b	nd	0.93
FL5.12-Akt (MTT)	0.42	5.7	1.7	2.3	0.20
MiaPaCa-2 (MTT)	0.59	13.3	10.8	3.18	0.1

^a Values are means of two or more experiments.

^b Not determined.

inhibitors were evaluated in MiaPaCa-2 human pancreatic cancer cells and FL5.12-Akt murine prolymphocytic cells that overexpress Akt1. As shown in **Table 4**, significantly less cellular activity was observed for compounds **10a**, **10e**, and **10o**. 3-Amino analog **10y** was statistically more active in both FL5.12-Akt and MiaPaCa-2 cells, correlating to its broader spectrum of kinase activity.

One of the major issues for use of compound **3** as an antitumor agent is its poor pharmacokinetic profile, including short half-life in most species (e.g., 0.3 h in mice), high plasma clearance, and lack of oral bioavailability. The C-1 position was identified as a major site of metabolism. As summarized in **Table 5**, substitution at the metabolically labile C-1 position with chlorine (**10l**) significantly increases half-life in mice (5 h). When administered orally in mice, this compound achieved respectable plasma exposure with a 3.9 μ g-h/mL AUC and 51% bioavailability (10 mg/kg dose). Introduction of a chlorine at C-3 position of the isoquinoline (**10p**) also improved the pharmacokinetic profile with an increased half-life in mice (2.0 h) and modest oral bioavailability (27%). No statistically significant difference was observed for a 3-amino group at the same position (**10y**). As we envisioned, the 1,8-steric influence from a C8-methyl group (**10aa**) indeed inhibited the metabolism of the isoquinoline, leading to a prolonged half-life (4.5 h vs 0.3 h for **3**) and 35% oral bioavailability. Unfortunately, all of these compounds with improved PK profiles suffered from diminished Akt activity.

Due to its overall profile in enzyme- and cellular assays as well as its PK property, **10y** was evaluated in a Mia-PaCa-2 human pancreatic cell xenograft model. Mia-PaCa-2 is a human pancreatic carcinoma line and it has been reported that the Akt signaling pathway is important in the pathogenesis of this tumor. As illustrated in **Figure 2**, at its maximally tolerated dose (75 mg/kg/day) for subcutaneous administration, this compound significantly slowed tumor growth. However, toxicity developed, including lethargy, weight loss and skin irritation at the site of injection after administration of the Akt inhibitor. All animals were humanely euthanized on day 27 due to the development of these toxicities.

In summary, substitution at the C-2 position of the pyridine in **3** could improve the selectivity against certain protein kinases. Chlorination at the C-1 site of metabolism or methylation at C-8 position of the isoquinoline resulted in compounds with improved pharmacokinetic properties, but diminished potency against Akt. 3-Amino analog **10y** was identified as a potent Akt inhibitor

Table 5. Mouse PK summary of representative Akt inhibitors^a

Compound	iv $t_{1/2}$ (h)	V_d (L/kg)	CL (L/h)	po F (%)	po AUC ($\mu\text{g}\cdot\text{h}/\text{mL}$)	sc AUC ($\mu\text{g}\cdot\text{h}/\text{mL}$)
3	0.3	7.0	19.5	0	0	7.6
10l	5	9.5	1.3	51	3.9	nd ^b
10p	2.0	15.5	5.4	27	0.91	nd
10y	0.7	11.8	12.1	0	0	6.9
10aa	4.5	16.4	2.5	35	1.5	nd

^a All pharmacokinetic studies shown in this table were carried out in CD1 mice with 3 mg/kg intravenous, 10 mg oral, and 30 mg subcutaneous dosing. Plasma samples were diluted with 2 volumes of acidified methanol, centrifuged at 11,000g for 5 min, and directly analyzed by UV–LC.

^b Not determined.

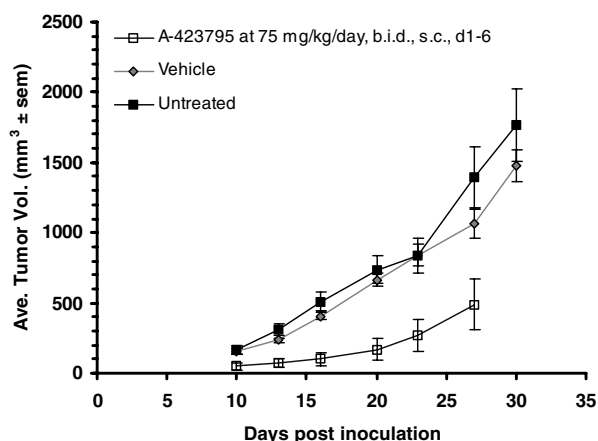


Figure 2. Analysis of **10y** (A-423795) in the MiaPaCa-2 xenograft pancreatic cancer model.¹⁰ **10y** was subcutaneously dosed at 75 mg/kg twice daily from day 1 to day 6 after inoculation. Tumor size was evaluated by twice weekly measurements with digital calipers. **10y** significantly inhibited tumor growth but also resulted in significant toxicity.

both in enzymatic and cellular assays. This compound significantly slowed tumor growth in vivo, but was accompanied by toxicity. The improved in vitro cytotoxicity of **10y** over **3** in a number of cell lines, as well as in vivo efficacy, seemed to correlate to its broader spectrum of activity against other protein kinases such as CDKs. Further profiling studies for this series of Akt inhibitors are underway and will be published in due course.

Acknowledgments

We thank Drs. Thomas Penning and Milan Bruncko for proofreading this manuscript and valuable suggestions.

References and notes

- For a review, see: Nicholson, K. M.; Anderson, N. G. *Cell. Signalling* **2002**, *14*, 381.
- For reviews, see: (a) Vivanco, I.; Sawyers, C. *Nat. Rev.* **2002**, *2*, 489; (b) Gills, J.; Dennis, P. *Expert Opin. Investig. Drugs* **2004**, *13*, 787.
- For review, see: (a) Li, Q.; Zhu, G.-D. *Curr. Top. Med. Chem.* **2002**, *2*, 939; (b) Barnett, S.; Bilodeau, M.; Lindsley, C. *Curr. Top. Med. Chem.* **2005**, *5*, 109.
- (a) Lindsley, C.; Zhao, Z.; Leister, W. H.; Robinson, R.; Barnett, S.; Defeo-Jones, D.; Jones, R.; Hartman, G.; Huff, J.; Huber, H.; Duggan, M. *Bioorg. Med. Chem. Lett.* **2005**, *15*, 761; (b) Barnett, S.; Defeo-Jones, D.; Fu, S.; Hancock, P.; Haskell, K.; Jones, R.; Kahana, A.; Kral, A.; Leander, K.; Lee, L.; Malinowski, J.; McAvoy, E.; Nahas, D.; Robinson, R.; Huber, H. *Biochem. J.* **2005**, *385*(Pt. 2), 399.
- Zhao, Z.; Leister, W.; Robinson, R.; Barnett, S.; Defeo-Jones, D.; Jones, R.; Hartman, G.; Huff, J.; Huber, H.; Duggan, M.; Lindsley, C. *Bioorg. Med. Chem. Lett.* **2005**, *15*, 905.
- (a) Luo, Y.; Shomaker, A.; Liu, X.; Woods, K.; Thomas, S.; de Jong, R.; Han, E.; Li, T.; Stoll, V.; Powlas, J.; Oleksijew, A.; Mitten, M.; Shi, S.; Guan, R.; McGonigal, T.; Klinghofer, V.; Johnson, E.; Levenson, J.; Bouska, J.; Mamo, M.; Smith, R.; Gramling-Evans, E.; Zinker, B.; Mika, A.; Nguyen, P.; Oltersdorf, T.; Rosenberg, S.; Li, Q.; Giranda, V. *Mol. Cancer Ther.* **2005**, *4*, 977; (b) Li, Q.; Woods, K.; Thomas, S.; Zhu, G.-D.; Packard, G.; Fisher, J.; Li, T.; Gong, J.; Dinges, J.; Song, X.; Abrams, J.; Luo, Y.; Johnson, E.; Shi, S.; Liu, X.; Klinghofer, V.; de Jong, R.; Oltersdorf, T.; Stoll, V.; Jakob, C.; Rosenberg, S.; Giranda, V. *Bioorg. Med. Chem. Lett.* **2006**, *16*, 2000.
- Koch, V.; Schnatterer, S. *Synthesis* **1990**, 499.
- Becker, M. R.; Ewing, W. R.; Davis, R. S.; Pauls, H. W.; Ly, C.; Li, A.; Mason, H. J.; Choi-Sledeski, Y. M.; Spada, A. P.; Chu, V.; Brown, K. D. *Bioorg. Med. Chem. Lett.* **1999**, *9*, 2753.
- Li, Q.; Woods, K.; Zhu, G.-D.; Fischer, J.; Gong, J.; Li, T.; Gandhi, V.; Thomas, S.; Packard, G.; Song, X.; Abrams, J.; Diebold, R.; Dinges, J.; Hutchins, C.; Stoll, V.; Rosenberg, S.; Giranda, V.; Colussi, D. J.; Leadley, R. J.; Bentley, R.; Bostwick, J.; Kasiewski, C.; Morgan, S. WO Patent 2003051366, 2005.
- Animal studies were conducted following the guidelines of the internal Institutional Animal Care and Use Committee. Immunocompromised male scid mice (C.B-17-Prkdc^{scid}) were randomly assigned to treatment groups and therapy was initiated the day after inoculation. Ten animals were assigned to each group, including controls. MiaPaCa-2 cells were obtained from the American Type Culture Collection (Manassa, VA). MiaPaCa-2 cells (2×10^6) in 50% Matrigel (BD Biosciences, Bedford, MA) were inoculated subcutaneously into the flank. Tumor size was evaluated by twice weekly measurements with digital calipers. Tumor volume was estimated using the formula: $V = L \times W^2/2$.